

A Supernova Factory in Mrk 273?

M. Bondi,¹ M-A. Pérez-Torres,² D. Dallacasa,³ T.W.B. Muxlow⁴

¹*INAF-Istituto di Radioastronomia, Via Gobetti 101, I-40129, Bologna, Italy*

²*Instituto de Astrofísica de Andalucía, CSIC, Apartado Correos 3004, 18080 Granada, Spain*

³*Dipartimento di Astronomia, Università di Bologna, Via Ranzani 1, I-40127 Bologna, Italy*

⁴*Jodrell Bank Observatory, University of Manchester, Macclesfield, Cheshire, SK119DL, U.K.*

10 November 2018

ABSTRACT

We report on 1.6 and 5.0 GHz observations of the ultraluminous infrared galaxy (ULIRG) Mrk 273, using the European VLBI Network (EVN) and the Multi-Element Radio-Linked Interferometer Network (MERLIN). We also make use of published 1.4 GHz VLBA observations of Mrk 273 by Carilli & Taylor (2000). Our 5 GHz images have a maximum resolution of 5–10 mas, which corresponds to linear resolutions of 3.5–7 pc at the distance of Mrk 273, and are the most sensitive high-resolution radio observations yet made of this ULIRG. Component N1, often pinpointed as a possible AGN, displays a steep spectral index ($\alpha = 1.2 \pm 0.1$; $S_\nu \propto \nu^{-\alpha}$); hence it is very difficult to reconcile with N1 being an AGN, and rather suggests that the compact nonthermal radio emission is produced by an extremely high luminous individual radio supernova (RSN), or a combination of unresolved emission from nested supernova remnants (SNR), luminous RSNe, or both. Component N2 is partly resolved out into several compact radio sources – none of which clearly dominates – and a region of extended emission about 30 pc in size. The integrated spectral index of this region is flat ($\alpha = 0.15 \pm 0.1$), which can be interpreted as due to a superposition of several unresolved components, e.g., RSNe or SNRs, whose radio emission peaks at different frequencies and is partially free-free absorbed. Is it also possible that one of the compact components detected in this region is the radio counterpart of the AGN. The overall extended radio emission from component N is typical of nonthermal, optically thin radio emission ($\alpha = 0.8 \pm 0.1$), and its 1.4 GHz luminosity ($L_{1.4\text{GHz}} = (2.2 \pm 0.1) \times 10^{23} \text{ WHz}^{-1}$) is consistent with being produced by relativistic electrons diffused away from supernova remnants in an outburst. The southern component, SE, shows also a very steep spectrum ($\alpha = 1.4 \pm 0.2$), and extended radio emission whose origin and physical interpretation is not straightforward.

Key words: galaxies: active – galaxies: individual (Markarian 273) – galaxies: starburst – supernovae: general

1 INTRODUCTION

Ultraluminous infrared galaxies (ULIRGs) are the most luminous galaxies in the local universe, with luminosities exceeding $10^{12} L_\odot$ (Sanders et al. 1988). ULIRGs are associated with merging systems, where large quantities of gas and dust are channeled in the inner regions and heated by a powerful source of optical-uv continuum. The most popular dust-heating mechanisms in ULIRGs propose the existence of either an active galactic nucleus (AGN), or a massive starburst, but which one is the dominant mechanism is hitherto an open question. Recent near-IR spectroscopic measurements suggest enhanced star formation in the majority of ULIRGs (Genzel et al. 1998), with a significant heating

from the AGN only in the most luminous objects (Veilleux, Sanders & Kim 1999).

Radio observations can prove to be extremely useful in shedding light to the relevant question of the dust-heating mechanism in ULIRGs, as they are unaffected by dust extinction and allow for sub-parsec resolution, using VLBI techniques. The most spectacular evidence to date of a dominant starburst in a ULIRG is the discovery of a population of bright radio supernovae (RSNe) in the nuclear region of Arp 220, detected at 1.6 GHz (Smith et al. 1998).

Mrk 273 is a ULIRG at $z = 0.0378$ ($D \simeq 150 \text{ Mpc}$ for $H_0 = 70 \text{ kms}^{-1}\text{Mpc}^{-1}$) classified as a Seyfert 2 and/or LINER merging system showing a disturbed morphology on the kpc scale. The nuclear region of Mrk 273 is extremely

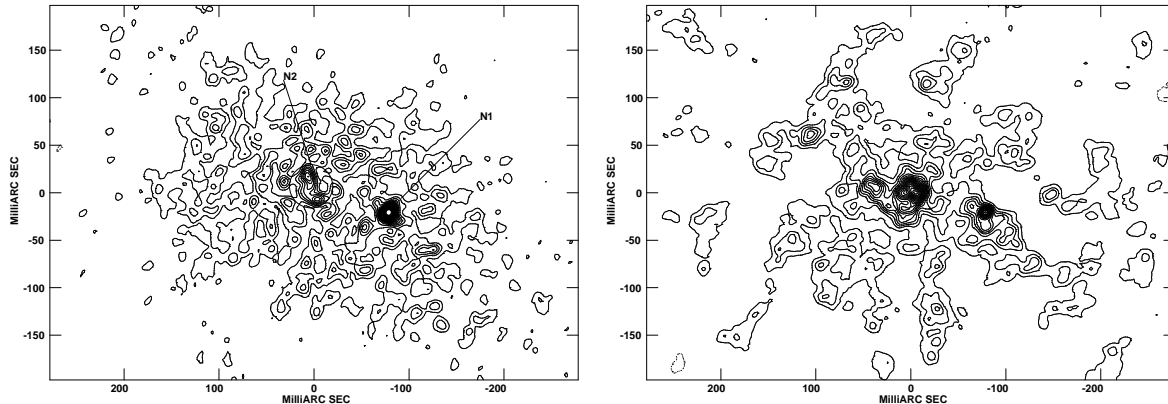


Figure 1. *a) Left:* Image of component N of Mrk 273 at 1.4 GHz at 10 mas resolution from Carilli & Taylor 2000. The contours are linear with an increment of 0.1 mJy/beam, starting at 0.1 mJy/beam. The peak surface brightness is 3.05 mJy/beam, and the off-source rms is 36 μ Jy/beam. Labels point to components discussed in the text. *b) Right:* Component N of Mrk 273 at 5 GHz, 10 mas resolution. The contours are $-1, 1, 2, 3, 4, \dots \times 0.04$ mJy/beam. The peak surface brightness is 0.74 mJy/beam and the off-source noise is 15 μ Jy/beam.

complex and has been studied in detail in the radio (Cole et al. 1999; Carilli & Taylor 2000, hereafter CT00; Yates et al. 2000), near infrared (Knäpen et al. 1997), optical (Mazzarella & Boroson 1993), and X-rays (Xia et al. 2002).

In this paper, we present high-resolution imaging (5–10 mas) of the 1.6 and 5 GHz continuum radio emission of Mrk 273, obtained with the European VLBI Network (EVN) and the Multi-Element Radio-Linked Interferometer Network (MERLIN). These data confirm the presence of an extremely strong starburst in component N, which we start resolving out in a large number of compact components, suggestive of a probable supernova factory in this region. The presence of a possible AGN in the nuclear environment of Mrk 273 is still elusive: its identification with component N1 is highly unlikely because of its radio spectrum; we also set up a stringent upper limit on the radio emission of an AGN nucleus in component SE. Despite the high sensitivity and milliarcsecond resolution of our observations, the nature of component SE is still unclear.

2 PREVIOUS HIGH RESOLUTION OBSERVATIONS OF THE NUCLEAR REGION IN MRK 273

Mrk 273 shows three extended radio components (conventionally named N, SE and SW, see Fig. 1 in Yates et al. 2000) within 1 arcsecond. These are physically related components, probably associated with the merging process, and not the result of chance projection of background sources. The three components show different morphologies and properties. Component SW is extended, of very low surface brightness and barely detected in the radio, while components N and SE are much brighter. In particular, component N shows two peaks, N1 and N2, embedded in extended radio emission. Component N and SW have bright NIR counterparts (Majewski et al. 1993; Knäpen et al. 1997) and are redder than component SE, suggesting the presence of strong star formation, while component SE is not detected in the NIR.

CT00 observed Mrk 273 in June 1999 at 1.4 GHz using the Very Long Baseline Array (VLBA) and the full Very

Large Array (VLA) to image component N and SE with 10 mas resolution. They resolved component N (Fig. 1a) in a number of compact features embedded in a weak and diffuse radio emitting region, and suggested that one of them, coincident with N1, could be associated with a weak AGN, while the other fainter compact features, mainly in a region around N2, could be nested SNR, luminous RSN, or both. While there is evidence for the presence of a weak AGN in component N (e.g., discovery of hard X-ray emission, Xia et al. 2002; OH megamaser emission, Klöckner & Baan 2004) the AGN cannot possibly account for more than a few percent of the observed radio emission.

The interpretation of the radio morphology of component SE is less straightforward: it shows (Fig. 3a) an elongated structure of about 40 mas long in the N-S direction, embedded in a weak halo, which is consistent with an amorphous jet or a very compact starburst. The lack of NIR emission in component SE could argue in favour of the AGN interpretation for this source, but the possibility that this component is still obscured at 2.2 μ m cannot be ruled out.

3 RADIO OBSERVATIONS

We observed Mrk 273 at 5 GHz using the EVN and MERLIN and at 1.6 GHz (EVN-only) in February 2004, with the main goal of performing a spectral analysis of the compact and extended features in the N and SE components. The observations were carried at 512 Mbit/s sustained bit rate to exploit the large bandwidth capabilities of the EVN, with an array which included all the European antennas. These were the first observations at 5 GHz for the resurfaced Lovell telescope. Mrk 273 was observed in phase-reference mode for a total on-source time of 5.5 hours at both frequencies. The compact source J1337+550 was observed every 5 minutes as phase reference, while OQ208 and J1310+322 were used to calibrate the bandpass. Data reduction was performed using the Astronomical Image Processing System (AIPS). Standard a priori gain calibration was performed using the measured gains and system temperatures of each antenna. The amplitude calibration was refined using the phase reference source. While the 5 GHz observations were of very

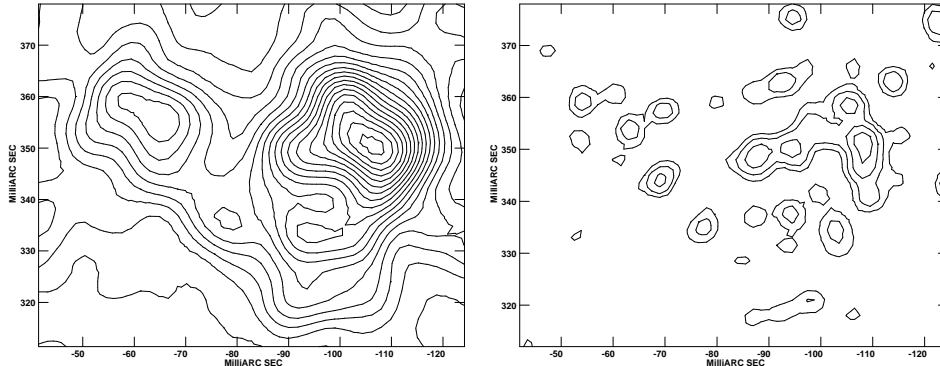


Figure 2. Blow out of the N2 region from the 5 GHz EVN+MERLIN image at 10 mas resolution (*left*) and 5 mas resolution (*right*). First contour in the 5 mas image is 0.1 mJy/beam.

high quality, the 1.6 GHz data suffered from failures in some of the large antennas, which prevented us from reaching the necessary accuracy and sensitivity to properly image the complex and extended emission in Mrk 273. For this reason, we resorted to use the 1.4 GHz observations obtained by CT00 in order to derive the spectral index properties of components N and SE. The 1σ r.m.s. noise is $15 \mu\text{Jy}$ and $36 \mu\text{Jy}$ for the EVN+MERLIN 5 GHz and EVN-only 1.6 GHz observations, respectively. Images at different frequencies were aligned using component N1.

4 DISCUSSION

4.1 The Northern Component

The northern source in Mrk 273 consists of two regions of compact emission, coincident with the N1 and N2 components of the lower resolution MERLIN image, embedded in a halo of diffuse emission of roughly the same extension of that detected at 1.4 GHz by Carilli & Taylor (see Fig. 1).

At this resolution the extended emission is heavily resolved, and the CLEAN algorithm tends to generate spurious compact sources when deconvolving diffuse emission regions. For this reason, a point-by-point comparison between the 1.4 GHz and 5 GHz images in the extended emission region is meaningless. On the other hand, the point-like component N1 and the region N2 (with a size of about 50 mas) are well defined and are likely not to be affected by deconvolution problems. It has been usually assumed in the literature that N1 hosts a weak AGN nucleus, while N2 is a very compact region of massive star formation. This view is supported by two major points: 1) the detection of high excitation IR lines (Genzel et al. 1998)) and hard X-ray emission (Xia et al. 2002) are evidences of an AGN-like nucleus in Mrk 273; 2) the CO emission and NIR peaks are spatially coincident with N2 (Knapen et al. 1997; Downes & Solomon 1998).

We find that component N1 has a very steep spectral index ($\alpha \simeq 1.2$; $S \propto \nu^{-\alpha}$) between 1.4 and 5 GHz, and a luminosity at 1.4 GHz of about $7 \times 10^{21} \text{ WHz}^{-1}$. The flux density of N1 derived from the lower quality 1.6 GHz observations (at the same epoch of the 5 GHz data) is consistent with a steep spectral index of about 1, so we can rule out that strong flux density variability between the CT00 obser-

vations in 1999 and ours in 2004 is responsible for the steep spectral index of component N1. While the radio luminosity falls in the range typical of radio nuclei in low luminosity AGNs and Seyfert galaxies (e.g. Falcke et al. 2000; Ulvestad & Ho 2001), the radio spectrum of these nuclei is, in the great majority of cases, flat or even inverted (Nagar, Wilson & Falcke 2001; Middelberg et al. 2004). On the other hand, the compact steep spectrum (CSS) and giga-Hertz peaked spectrum (GPS) sources have compact pc-scale morphology and steep radio spectrum but are 3-4 orders of magnitude more luminous than N1 (O’Dea 1998). Such properties are difficult to reconcile with N1 being an AGN, and rather suggests a supernova origin for the nonthermal radio emission. The steep spectral index is indeed typical of a young RSN (e.g., Weiler et al. 2002), but in this case it would be an extremely luminous one. In fact, the average maximum luminosity of typical radio supernovae is around $2 \times 10^{20} \text{ WHz}^{-1}$, and the most luminous type II in radio SN, like SN1988Z, are still a factor of three to four less luminous at maximum than N1. Given this premise, a realistic scenario would be one in which N1 is not an individual radio SN, but a combination of nested supernova remnants, several luminous radio supernovae, or both. Higher resolution multifrequency observations are needed to clarify the nature of component N1.

Component N2 shows a more complex morphology. It occupies a well defined region of about 50 mas in size, partly resolved into several compact radio sources, whose integrated spectral index is flat ($\alpha \simeq 0.15$). Such a flat spectrum could be due to a superposition of several, unresolved components whose radio emission peaks at different frequencies and is partially free-free absorbed. In Figure 2 we show a blow out of the N2 region, obtained with a resolution of 10 mas and 5 mas. In the full resolution image, we resolve most of the emission in N2 in compact features which we tentatively identify with RSN and/or SNR. These compact features are weak (peak brightness in the range 0.1-0.4 mJy/beam) and the possibility that some of them might be spurious components, produced by resolving out the extended emission in N2, cannot be excluded. On the other hand, we note that most of these compact features can be identified in the 10 mas resolution image as well, where the N2 region is not resolved out or affected by deconvolution problems. In order to test the fidelity of the flux density measurements of the compact features in

our images we ran the following test. We added, in the u - v plane, 10 point-like components in the central region of Mrk 273 N with random positions and peak flux densities in the range 0.1–0.4 mJy/beam using the task UVMOD in AIPS. We then cleaned the image in the same manner as we did for the image shown in Fig. 2b, and derived the peak flux of the components previously injected. We repeated this exercise 30 times, obtaining a sample of 300 simulated sources. For each source we derived the difference between the measured and real flux normalized by the r.m.s. noise (σ). Only 14/300 (4.6%) and 55/300 (18%) sources have measured fluxes which are different from the real values by more than 3σ and 2σ , respectively. Considering we injected these sources in an area where other components are already present, and that we did not make any attempt to discriminate among these cases, the test reassures us about the fidelity of the flux densities of the compact components derived from the images.

The radio morphology of the region N2 suggests the presence of multiple compact components in an area of about 30 pc of size, and this is also consistent with the results from CO and NIR emission observations which indicate this region as the core of an extremely rich star forming region.

Downes & Solomon (1998) derived an IR luminosity of $6.0 \times 10^{11} L_{\odot}$ generated in a region of radius ~ 120 pc around components N1 and N2, and estimated a molecular mass of $\approx 1.0 \times 10^9 M_{\odot}$, and a mass in new stars (i.e., excluding matter lost from the earliest high-mass stars during their post-main-sequence evolution) of $M_{\star} \approx 1.6 \times 10^9 M_{\odot}$. The above values are useful to constrain scenarios in which the luminosity in the nuclear region of Mrk 273 arises from a starburst. We follow here the prescription by Scoville, Yun & Bryant (1997), which characterize a starburst by its total luminosity, L , Ly continuum production, Q , and accumulated stellar mass, M_{\star} . Those values are obtained as power-law approximations of the lower and upper mass cut-offs for stars, m_l and m_u , the constant rate of star formation, \dot{M} , and the burst timescale, t_B . In particular, for a burst timescale of $t_B = 5 \times 10^7$ yr a simultaneous match for the values of L_{FIR} and M_{\star} yields $m_l \approx 3.0 M_{\odot}$, $m_u \approx 30 M_{\odot}$, and $\dot{M} \approx 39 M_{\odot} \text{ yr}^{-1}$. The implied ionizing photon rate is $Q \approx 3.9 \times 10^{44} \text{ s}^{-1}$, about a factor of two smaller than for Arp 220. Here, we used a minimum mass for yielding type II supernovae of $8 M_{\odot}$, which results in a supernova rate $\nu_{\text{SN}} \approx 1.3 \text{ yr}^{-1}$. (For longer burst timescales, e.g., $t_B = 10^8$ yr, the upper mass limit can be increased to about $35 M_{\odot}$, while \dot{M} can be decreased to $\approx 31 M_{\odot}$, implying a supernova rate of $\approx 1.0 \text{ yr}^{-1}$.) Starbursts with very low-mass stars ($m_l = 0.1 M_{\odot}$) can probably be ruled out, as they require a mass in stars about an order of magnitude greater than expected.

We also used our radio flux density measurements of component N to constrain the range of plausible models for a starburst in Mrk 273. The extended radio emission of the northern component has a total flux of ~ 80 mJy at 1.4 GHz, and an average spectral index between 1.4 and 5 GHz of $\alpha \approx 0.8$, yielding an observed luminosity $L \simeq 2.2 \times 10^{23} \text{ W Hz}^{-1}$. Condon (1992) gives a number of simple scaling law relationship to estimate starburst characteristics in terms of only one free parameter, namely the star formation rate of stars more massive than $5 M_{\odot}$. Using the same scalings as in Scoville et al. 1997, but setting the

minimum mass for the star forming rate to $5 M_{\odot}$, we obtain $\dot{M}(M \geq 5 M_{\odot}) \approx 32 M_{\odot} \text{ yr}^{-1}$, which yields $\nu_{\text{SN}} \approx 1.5 \text{ yr}^{-1}$. Such a supernova rate would produce a non-thermal (synchrotron) luminosity of $L_{\text{syn}} \approx 1.5 \times 10^{23} \text{ W Hz}^{-1}$ at 1.4 GHz, which is about a 30% lower than the observed value. The star formation rate should be $\dot{M}(M \geq 5 M_{\odot}) \gtrsim 40 M_{\odot} \text{ yr}^{-1}$ to be within 3σ of the observed extended radio emission at 1.4 GHz ($3\sigma \approx 0.4 \times 10^{23} \text{ W Hz}^{-1}$), and would imply $\nu_{\text{SN}} \approx 2.0 \text{ yr}^{-1}$ (Condon 1992). In turn, this would imply a L_{FIR} for component N of $7.7 \times 10^{11} L_{\odot}$. Since the total L_{FIR} for Mrk 273 is about $1.2 \times 10^{12} L_{\odot}$, and given that DS98 do not provide quantitative estimates of the uncertainty for L_{FIR} of N, the above value for L_{FIR} is acceptable. Therefore, the observed extended radio emission is easily explained within those models and supports a scenario where it is due to relativistic electrons that have diffused away from SNR shocks. Given the existing uncertainties, we estimate that a supernova rate of $\nu_{\text{SN}} = 1.5 \text{ yr}^{-1}$ is likely to apply for Mrk 273, within an uncertainty of a factor of 2. A radio supernova would thus explode in the northern component of Mrk 273 approximately every eight months, and several supernovae would have been exploded between the observations of CT00 on 1999, and ours in 2004.

4.2 The South-Eastern Component

It has been suggested that component SE is a background source unrelated to Mrk 273, based on the lack of an NIR counterpart to component SE (Knapen et al. 1997). However, as already pointed out by CT00, the chances of having a background source of ~ 40 mJy at an angular distance of 0.8 arcsec from component N are less than 5×10^{-7} . The 1.4 GHz images do not clarify whether the source is core-jet, hence AGN driven, or a compact starburst, and observations in other bands do not provide a unique interpretation. At 5 GHz, the SE component is resolved in an arc-shaped radio emission resembling a core twin-jet source. The most striking peculiarity of the SE component is its steep spectral index. The integrated value is $\alpha \simeq 1.4$ with values ranging from 0.9 to 1.6 across the source. At the full resolution of the EVN observations (5 mas) the source is completely resolved out, thus confirming the absence of any high brightness radio feature and arguing against component SE being an AGN. In particular, given a 5σ limit of 0.13 mJy, we set an upper limit of $4 \times 10^{20} \text{ W Hz}^{-1}$ for the 5 GHz radio luminosity of any AGN in this region. One possibility could be that SE hosts also a compact starburst. However, in that case we should expect the existence of diffuse emission in an extended region. Instead, both the 1.4 GHz image of CT00 and our 5 GHz image (see Fig. 3) show component SE to be rather compact, yet morphologically very much different. This frequency dependent morphology should not exist if we were dealing with a starburst scenario. Hence, despite the milliarcsecond resolution and high sensitivity of our new images, the physical nature of component SE remains elusive, and unveiling it will have to await until more sensitive, multi-band observations are carried out.

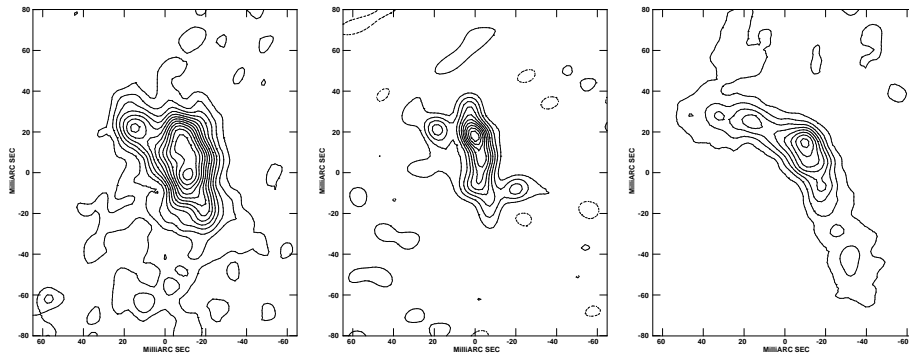


Figure 3. Component SE in Mrk 273 imaged with a 10 mas beam. *a) Left:* VLBA+VLA at 1.4 GHz (June 1999), contours and noise as fig. 1a; *b) Middle:* EVN at 1.6 GHz (Feb 2004), first contour 0.11 mJy/beam linear increment, noise 35 μ Jy/beam. *c) Right:* EVN+MERLIN at 5 GHz (Feb 2004), contours and noise as fig. 1b.

5 SUMMARY

We have presented the results from the most sensitive high-resolution observations of the nuclear region in the ULIRG Mrk 273 ever made. Previous observations supported the scenario of a weak AGN and an extremely luminous starburst coexisting in the nucleus of Mrk 273. We tested this hypothesis using our new VLBI data at 1.6 and 5 GHz together with the 1.4 GHz images published by CT00.

The main results of our analysis can be summarized as follows:

(i) Component N1, previously pinpointed as the radio counterpart of the AGN, displays a steep spectral index between 1.4 and 5 GHz ($\alpha = 1.2 \pm 0.1$; $S_\nu \propto \nu^{-\alpha}$). Given the steep radio spectrum is highly unlikely that N1 is hosting the AGN, and it rather suggests that the compact non-thermal radio emission is produced by an individual RSN (which would then be three to four times more luminous than SN 1988Z), or by a combination of unresolved emission from several nested SNR and/or RSN.

(ii) Component N2 displays both a rather complex and intriguing morphology and spectral properties. The 5 GHz radio image is indicative of several compact features embedded in some diffuse emission extended over a region of about 30 pc. The integrated spectral index of this region is flat ($\alpha = 0.15 \pm 0.10$), which can be interpreted as due to the superposition of several unresolved components, e.g., RSNe, SNR, or both, whose radio emission peaks at different frequencies and is partially free-free absorbed. Is it also possible that one of the compact components in this region is the radio counterpart of the AGN.

(iii) The radio morphology of component N as a whole supports the hypothesis that this is indeed the site of an extremely active star forming region. Following Scoville et al. (1997), and using the constraints on the IR luminosity from the inner 120 pc central region around the nucleus (Downes & Solomon 1998), a starburst lasting for $t_B = 5 \times 10^7$ yr, with a Miller-Scalo initial mass function characterized by $m_l \approx 3.0 M_\odot$, $m_u \approx 30 M_\odot$, and a sustained star formation rate of $\dot{M} \approx 39 M_\odot \text{ yr}^{-1}$ can easily yield the observed FIR and radio emission. Such a starburst would result into an estimated supernova rate for Mrk 273 of $\nu_{SN} \approx 1.5 \text{ yr}^{-1}$, and thus several supernovae would have

exploded between the observations of CT00 on 1999, and ours in 2004.

(iv) The extended radio emission in component N has the typical spectral index of non-thermal, optically thin emission ($\alpha = 0.8 \pm 0.1$), and luminosity ($L_{1.4\text{GHz}} = (2.2 \pm 0.1) \times 10^{23} \text{ W Hz}^{-1}$) consistent with being produced by relativistic electrons diffused away from supernova remnants in a recent outburst.

(v) Finally, the origin and interpretation of the radio emission from Mrk 273 SE remains unclear. It has a very steep spectral index ($\alpha = 1.4 \pm 0.2$), with no compact and/or flat spectrum feature. This would favour a starburst origin for the radio emission, although the lack of NIR emission poses some problems.

ACKNOWLEDGMENTS

We thank Chris Carilli for having kindly provided the processed VLBA images at 1.4 GHz of Mrk 273, and the staff at JIVE for the efforts spent during the correlation and pipeline of these data. This work has benefited from research funding from the European Community's Sixth Framework Programme (FP6). The European VLBI Network is a joint facility of European, Chinese, South African and other astronomy institutes funded by their national research councils. MERLIN is a national facility operated by the University of Manchester on behalf of PPARC. This research has made use of the NASA/IPAC Extragalactic Database (NED) which is operated by the Jet Propulsion Laboratory, California Institute of Technology, under contract with the National Aeronautics and Space Administration.

REFERENCES

- Carilli, C.L., Taylor, G.B., 2000, ApJ, 532, L95 (CT00)
- Cole, G.H.J., Pedlar, A., Holloway, A.J., Mundell, C.G., 1999, MNRAS, 310, 1033
- Condon, J.J., 1992, ARAA, 30, 575
- Downes, D., Solomon, P.M., 1998, ApJ, 507, 615
- Falcke, H., Nagar, N.M., Wilson, A.S., Ulvestad, J.S., 2000, ApJ, 542, 197
- Genzel, R. et al. 1998, ApJ, 498, 579
- Klöckner, H.-R., & Baan, W.A., 2004, A&A, 419, 887

- Knapen, J.H., Laine, S., Yates, J.A., Robinson, A., Richards, A.M.S., Doyon, R., Nadeau, D., 1997, *ApJ*, 490, L29
- Majewski, S.R., Hereld, M., Koo, D.C., Illingworth, G.D., Heckman, T.M., 1993, *ApJ*, 402, 125
- Mazzarella, J.M., Boroson, T.A., 1993, *ApJS*, 85, 27
- Middelberg, E., et al. 2004, *A&A*, 417, 925
- Nagar, N.M., Wilson, A.S., Falcke, H., 2001, *ApJ*, 559, L87
- O'Dea, C.P., 1998, *PASP*, 110, 493
- Sanders, D.B., Soifer, B.T., Elias, J.H., Madore, B.F., Matthews, K., Neugebauer, G., Scoville, N.Z., 1988, *ApJ*, 325, 74
- Scoville, N.Z., Yun, M.S., Bryant, P.M., 1997, *ApJ*, 484, 702
- Smith, H.E., Lonsdale, C.J., Lonsdale, C.J., Diamond, P.J., 1998, *ApJ*, 493, L17
- Ulvestad, J.S., Ho, L.C., 2001, *ApJ*, 558, 561
- Veilleux, S., Sanders, D.B., Kim, D.C., 1999, *ApJ*, 522, 113
- Weiler K. W., Panagia N., Montes M. J., Sramek R. A., 2002, *ARA&A*, 40, 387
- Xia, X.Y., Xue, S.J., Mao, S., Boller, Th., Deng, Z.G., Wu, H., 2002, *ApJ*, 564, 196
- Yates, J.A., Richards, A.M.S., Wright, M.M., Collett, J.L., Gray, M.D., Field, D., Cohen, R.J., 2000, *MNRAS*, 317, 28